Intertube interactions in carbon nanotube bundles

Ágnes Szabados,[1,*] László P. Biró,[2,†] and Péter R. Surján[1,‡]
[1]*Loránd Eötvös University, Department of Theoretical Chemistry, H-1518 Budapest, P.O. Box 32, Hungary*
[2]*Research Institute for Technical Physics & Materials Science, H-1525 Budapest, P.O. Box 49, Hungary*
(Received 27 January 2006; revised manuscript received 10 March 2006; published 5 May 2006)

Energetics of pairs and seven membered bundles formed by achiral as well as chiral carbon nanotubes is explored. The applied model Hamiltonian consists of a tight binding intratube part, an intermolecular hopping term, and a Lennard-Jones pair potential. Heterochiral aligned tube pairs are found the most stable energetically. Rotation of tubes around the tube axis in an aligned pair of identical tubes requires the smallest energy input if a cog-wheel rotation (disrotation) is exercised for heterochiral and achiral pairs or anti-cog-wheel rotation (conrotation) for a homochiral pair. Energetic preference for disrotation in heterochiral identical pairs manifests even for short (several nanometer long) tubes. Conrotation of homochiral pairs is hindered by end effects and becomes favorable only if modeling long (infinite) identical tubes. Among achiral tubes, those that possess a C_{3n} axis with odd n are shown to form close-packed bundles in an energetically optimal way. Similarly, among achiral tubes those having a C_{3n} axis, n either even or odd can form an energetically favorable close-packed bundle.

DOI: 10.1103/PhysRevB.73.195404 PACS number(s): 61.46.Fg

I. INTRODUCTION

Beyond their remarkable electronic properties,[1] carbon nanotubes[2] have excellent mechanical properties too.[3] For many practical applications, like fibers,[4,5] yarns,[6] self-supporting sheets,[7] etc., carbon nanotubes have to be assembled in macroscopic objects in order to exploit the very advantageous strength to density ratio of carbon nanotubes (100 times higher than for steel),[8] or their capacity to carry high electric current densities[9] of the order of 10^9 Å/cm^2. Insofar several approaches to this problem have been taken: solubilizing the carbon nanotubes using surfactants followed by the removal of the surfactant and coagulation of the suspension into fibers,[4] direct drawing of fibers or sheets from vertically aligned carbon nanotube forests,[7] etc. Ultimately, all these techniques end up with carbon nanotubes held together by van der Waals forces in a similar way like bulk graphite or carbon nanotube bundles produced during growth. Therefore bundle formation is not only interesting from the point of view of understanding the growth of single wall carbon nanotubes (SWCNTs), but for practical applications, too.

Bundle formation during growth and the possible role which the van der Waals interaction may play during the process is important for understanding the way in which SWCNTs are formed. Bundle formation during growth may equally be a desired or a highly undesired process: if fibers are to be manufactured, bundles are helpful. On the other hand, if a good dispersion of individual nanotubes—for composite applications—is to be achieved, bundles are highly undesirable. The difficulty to achieve good dispersion is a direct proof of the strength and importance of the van der Waals interaction of carbon nanotubes.

Recent studies by electron diffraction showed that in bundles of SWCNTs grown by chemical vapor deposition methods (CCVD), the nanotubes tend to have the same chirality and similar diameter.[10] The comparison of the bundles grown by CCVD, laser ablation, and by the arc method showed that while in the first two, indeed the bundles are smaller in diameter and tend to have the same chirality and similar diameters, in the case of arc growth the situation is different.[11] One of the possible reasons for this may be associated with the preferential nucleation and growth of homochiral bundles in those processes in which less turbulence is involved in the region where the nanotubes grow. In an earlier work[12] we investigated the effects that may arise from the van der Waals interaction of SWCNTs of similar diameter. In this work the atomic details of the structure were disregarded. We found that the magnitude of the van der Waals interaction of structureless tubes is too small for having a significant influence on the preferential nucleation.[12] In the present work we investigate in detail effects that may arise from the interactions of SWCNTs of similar diameter taking into account the atomic structure. We use a tight-binding formalism for intramolecular (intratube) interaction and an all pair model for intermolecular one electron hopping. The quantum-mechanical part of the calculation is augmented by an intertube Lennard-Jones potential. Interaction of several families of tubes of diameters close to the (10,10) tube are computed. Both homochiral (left-handed–left-handed) and heterochiral (left-handed–right-handed) arrangements are considered for tube pairs.

II. THEORETICAL DESCRIPTION OF INTERACTING CNTS

Tight-binding description of extended conjugated systems like fullerenes or carbon nanotubes (CNTs) has been frequently and successively applied to compute several properties of such systems. Augmented with a Lennard-Jones-type expression to account for intercluster interactions, the tight-binding model has been useful to characterize weakly interacting CNTs forming bundles[13,14] or multiwall tubes.[15,16] In the present work the tight-binding philosophy is generalized to apply both to intra- and intermolecular interactions, lead-

ing to the intermolecular Hückel (IMH) model introduced in Ref. 17. Intersystem hopping, applied also in other models,[18–20] offers the possibility to put more emphasis on orientational effects in intersystem interaction than it is possible by a mere scalar pair potential. On the other extreme, a Hückel model has the advantage over *ab initio* treatment in being (i) much simpler and easier to solve and (ii) applicable to relatively large molecular clusters.

A quick account of the theory is as follows. Intrasystem hopping

$$H^{\mathrm{A}} = \sum_{\mu<\nu}^{\text{neighbors on A}} \beta_{\mu\nu}(a_\mu^+ a_\nu + a_\nu^+ a_\mu) \tag{1}$$

is taken to characterize an isolated CNT called A, while the interaction between CNTs A and B is accounted for by the intersystem hopping term

$$H^{\mathrm{AB}}_{\mathrm{hopping}} = \sum_{\mu}^{\mathrm{A}} \sum_{\nu}^{\mathrm{B}} t_{\mu\nu}(a_\mu^+ a_\nu + a_\nu^+ a_\mu) \tag{2}$$

and by a sum of 6–12 pair potentials

$$E^{\mathrm{AB}}_{\text{Lennard-Jones}} = \sum_{\mu}^{\mathrm{A}} \sum_{\nu}^{\mathrm{B}} \left(\frac{A_{12}}{r_{\mu\nu}^{12}} - \frac{A_6}{r_{\mu\nu}^{6}} \right), \tag{3}$$

with $r_{\mu\nu}$ referring to the distance between sites μ and ν. The scalar Lennard-Jones term does not enter the quantum-mechanical part of the calculation. The total Hamiltonian corresponding to an interacting pair of CNTs AB is

$$H^{\mathrm{AB}} = H^{\mathrm{A}} + H^{\mathrm{B}} + H^{\mathrm{AB}}_{\mathrm{hopping}} + E^{\mathrm{AB}}_{\text{Lennard-Jones}} \tag{4}$$

with straightforward generalization to more than two interacting partners.

Parameters $\beta_{\mu\nu}$, $t_{\mu\nu}$, A_6, and A_{12} are set according to the following scheme. Intrasystem hopping parameter $\beta_{\mu\nu}$ scales down exponentially with increasing site-site distance

$$\beta_{\mu\nu} = -\beta_0 e^{-\zeta r_{\mu\nu}} \tag{5}$$

with $\beta_0 = 243.504\,86$ eV and $\zeta = 0.307\,451\,8$ Å^{-1}. These values are determined to give 1.5-eV gap and 1.36/1.45 Å bond length alternation for poliacetylene.[21] The first singlet transition of benzene by these parameter values is 5.1 eV as compared to the experimental 4.7–5.2 eV.[22,23] This parametrization was successfully used in several studies on conjugated systems.[24,25] Intersystem hopping parameter $t_{\mu\nu}$ is proportional to the overlap integral of p_z orbitals perpendicular to the molecular sheet,[37] centered on sites μ and ν,

$$t_{\mu\nu} = -t_0 S_{\mu\nu} \tag{6}$$

with $t_0 = 18.095\,66$ eV. The exponential decay of the overlap integral $S_{\mu\nu}$ is characterized by the Slater exponent of the carbon atom, 2.895 Å^{-1}. Parameters of the Lennard-Jones potential are $A_6 = 43.676\,642$ eV Å^6, and $A_{12} = 88\,817.6245$ eV Å^{12}.

The three parameters t_0, A_6, and A_{12} that affect the description of the interaction of molecules are fitted on interacting conjugated systems so as to reproduce the following:

(i) The difference in the interaction energies of two naphthalene molecules computed *ab initio* by second-order perturbation theory in the Møller-Plesset partitioning in the 6−31G* basis set. A 0.1-eV interaction energy difference results between the two arrangements where naphthalene molecules imitate either *AB* or *AA* stacking of graphite.

(ii) Energy minimum at 3.43-Å intersheet distance for two interacting graphitic segments in *AB* stacking.

(iii) Energy minimum at 3.6-Å intersheet distance of two interacting graphitic segments in *AA* stacking.

At step (i) the value of t_0 was determined, utilizing purely the hopping terms of the IMH Hamiltonian. Steps (ii) and (iii) together set the van der Waals parameters A_6 and A_{12}, at a t_0 value already fixed from step (i). This parametrization results a 0.4-meV per atom barrier to inner tube rotation for a five unit cell $(5,5)@(10,10)$ double wall carbon nanotube (DWCNT) segment, which compares well with the 0.8-meV per atom barrier obtained by Kwon and Tománek.[15]

Since diagonalization of the IMH Hamiltonian Eq. (4)—that would mean the exact solution of the model—is too demanding for the systems studied here, a perturbation theory (PT) based strategy is applied. Isolated system Hamiltonians $H^A + H^B$ are considered as zero order, and the effect of the interaction term $H^{AB}_{\mathrm{hopping}}$ is calculated up to second order in PT. Computation of the perturbation correction due to intersystem hopping interactions is speeded up tremendously by writing energy denominators as Laplace transforms[26] in the PT formulas, leading to a linear-scaling $[\mathcal{O}(N)]$ formulation. By factorizing the energy denominators, Laplace transform leads to effective intermediers thereby opening a way to a fast scan of potential hypersurfaces of interacting molecules. It is to be noted that fast computation of the interaction energy is possible only if the geometries of the interacting partners are kept rigid.

Compared to the exact solution of the model, second-order PT gives potential energy barriers with an acceptable, 5% error, according to test calculations performed on short segments of interacting nonmetallic CNTs, i.e., CNTs with nonzero gap.

III. RESULTS

To understand the apparent preference for same diameter and helicity in, e.g., CCVD bundles is a challenging task for theory. By studying the energetics of pairs and small bundles in this study an initial step is taken in this line. A similar study on the energetics of relative motion of DWCNT walls obtained by density-functional theory has been recently reported.[27] Dynamics and statistical properties as temperature are not considered presently. The reported interaction energies correspond to defect free CNTs.

In most of the cases studied, computation for a common unit cell of incommensurate CNTs forming pairs or bundles was not possible. Therefore, in addition to bulk tube-tube interaction, end effects are also reflected in the computed results. To obtain similar effect of the tube ending in finite-size calculations, a common tube length is fixed in calculations that are to be compared.

In Sec. III A pairs of $(10,10)$ and $(11,9)$, $(15,4)$, $(12,8)$, $(17,1)$ tubes are examined, the latter four being close to

(10,10) in diameter. (Diameters are 13.46, 13.49, 13.49, 13.55, and 13.62 Å, respectively.) Tube endings were left open in all calculations, merely dangling bonds (i.e., sites having just one neighbor) were removed at the ends to avoid the appearance of zero energy states in the spectrum of isolated tubes. To allow comparison with experimental observations, pairs of (10,10) and (13,7) tubes found in CCVD bundles and (14,5), (12,6), (10,9) tubes found in laser ablation produced bundles[11] are also computed, within the same circumstances as detailed above.

In one example infinitely long tubes are modeled, in order to remove end effects. This is performed by imposing periodic boundary conditions on the Hamiltonian matrix of a single unit cell, which corresponds to a single point band-structure calculation at $k=0$.

In Sec. III B seven membered bundles of finite tubes are constructed so that six aligned tubes form a regular hexagon and a seventh tube occupies the middle. The geometry of this arrangement is specified by seven rotation angles and a distance parameter. Rotational angles in these bundles correspond to a local minimum on the potential hypersurface in all cases.

In spite of the fact that barriers to relative motion of interacting CNTs with incommensurate walls do not grow monotonically with increasing tube length,[28] we report interaction energies and barriers divided by either tube length or interacting surface area in order to obtain comparable figures.

A. Pairs of CNTs

1. Rotational potential surfaces

Rotational potential surface of aligned pairs of similar diameter CNTs were explored, rotating each tube around its own axis. The CNTs considered are all chiral, apart from the (10,10) tube. For each pair of chiral tubes two different complexes were examined: a homochiral pair (i.e., two left-handed or two right-handed tubes, abbreviated as *rr*) and a heterochiral pair (i.e., a left- and a right-handed tube, abbreviated as *rl*).[38]

Typical examples for interaction energies as a function of the two rotation angles α and β are shown in Fig. 1 for identical tubes and in Fig. 2 for nonidentical tubes. The homo- and heterochiral situations are plotted on a common scale in Fig. 2. In the case of an identical pair the energetics is markedly different for the homo- and heterochiral complex. The corrugation of the surface (i.e., maximum variation of the energy as the tubes are rotated all around) in Fig. 1 is five times larger than the same quantity for the homochiral complex: 26.5 meV/Å compared to 5.2 meV/Å. The homochiral potential surface [shown in Fig. 4(a)] would therefore look flat on a common scale with the heterochiral complex in Fig. 1.

The regular, stripy pattern of Fig. 1 indicates that a heterochiral identical pair is the easiest to rotate if turning both tubes with the same angle in opposite direction (cog-wheel rotation or disrotation). To understand this phenomenon unit cells are unwrapped as visualized in Fig. 3, a vertical window indicating the original facing area. Upon disrotation the window is shifted either to the left or to the right. Such a displacement has practically no effect in Fig. 3(a), that shows the heterochiral situation, with a favorable *AB*-like stacking of the unit cells. This arrangement gives rise to large interaction stripes (valleys) in Fig. 1, while at small interaction stripes (ridges) the two unit cells in Fig. 3(a) are shifted with respect to each other to recover an *AA* kind of stacking. In the homochiral case depicted in Fig. 3(b), the two unit cells are mirror images of each other, a repeating pattern therefore cannot be formed within the unit cell. This leads to a more leveled surface in the homochiral case than for the heterochiral complex.

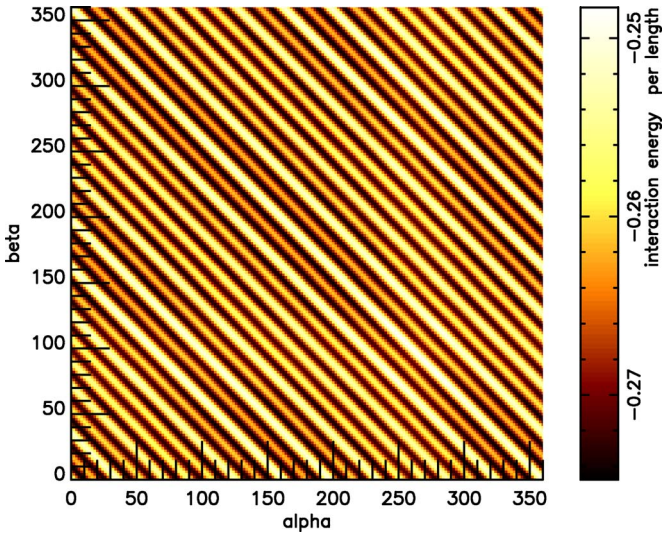

FIG. 1. (Color online) Rotational potential surface of two aligned (11,9) tubes, *rl* pair. Length of tubes is 73.4 Å, there are 1202 atoms per tube, wall to wall distance is 3.17 Å. Dimension of figures is eV/Å.

For the (10,10)||(10,10) pair Kwon *et al.*[14] reported a stripy surface similar to Fig. 1, obtained by a tight-binding model with an additional pairwise interatomic energy term. According to their calculation, small interaction stripes are broken up for peaks isolated by minima as deep as the other deep regions of the surface. This qualitative disagreement with the present calculation stems from the orientational effects included by the intersystem hopping term Eq. (2). Our control calculations show that these effects are entirely missing if describing intertube interaction solely by a Lennard-Jones potential Eq. (3), producing a rotational potential surface that agrees well the calculation of Kwon *et al.*

A pair of nonidentical tubes (Fig. 2) shows less regularity than the potential surface of identical aligned pairs. There are deep and high regions superimposed on a stripy pattern less expressed than in Fig. 1. Local minima at around $\alpha=50°+k90°$ and local maxima at around $\beta=90°$ in Fig. 2(a) result from the nonperpendicular cut of the tube at its ending. Certainly, the end effect is also present for identical heterochiral pairs, but there it is overwhelmed by the energy scale broadening due to the formation of regular patterns.

Comparison of the finite molecular treatment with a calculation imposing periodic boundary conditions presented in Fig. 4 makes it possible to pick out the effect of tube ending.

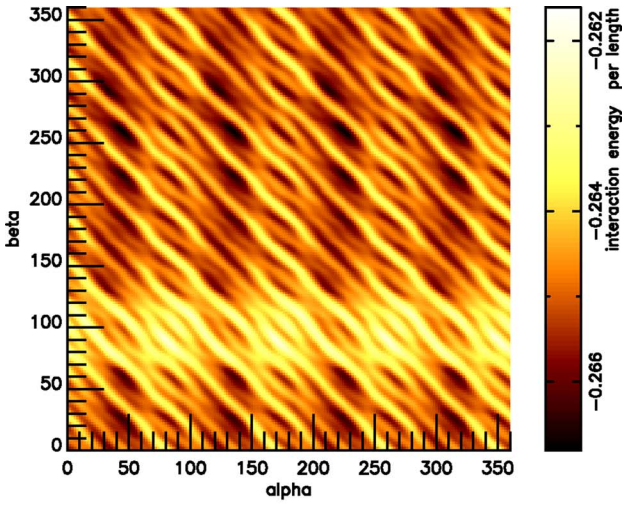

(a)

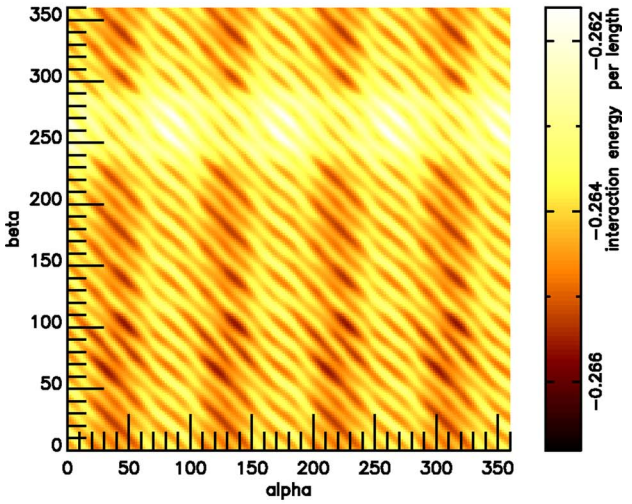

(b)

FIG. 2. (Color online) Rotational potential surface of a pair of aligned (12,8) and (11,9) tubes, (a) *rl* pair, (b) *rr* pair. Length of tubes is 73.4 Å, there are 1208 and 1102 atoms, respectively, wall to wall distance is 3.13 Å. Dimension of figures is eV/Å.

For endless tubes [Fig. 4(b)] local minima [at around $\alpha = 80°$ and $\beta = 270°$ in Fig. 4(a)] disappear, revealing a stripy pattern similar to Fig. 1. An important difference between Fig. 4(b) and Fig. 1 is that stripes have a positive slope for the homochiral pair. Hence infinite homochiral pairs are easy to rotate if turning both tubes with the same angle in the same direction (anti-cog-wheel rotation or conrotation). This rotation corresponds to fixing the vertical window in Fig. 3(b) and shifting one sheet to the left and the other to the right, by the same amount. It is also notable, that the corrugation is approximately six times larger for the heterochiral identical pair (Fig. 1) than for the homochiral complex [Fig. 4(b)].

The significant differences found between the calculations taking into account tube ends [Fig. 4(a)]—"short tubes" and

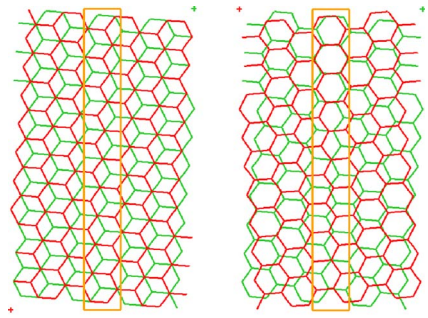

(a) (b)

FIG. 3. (Color online) Unit cells of two (4,3) tubes, set so that wrapping up in opposite directions results a heterochiral pair (a) or homochiral pair (b). Vertical window indicates the facing of the aligned tubes produced upon wrapping the sheets.

calculations with periodic boundary conditions [Fig. 4(b)]—"infinitely long tubes"—indicate that during the early phases of nucleation and growth the defects associated with tube ends may have a marked influence in making a certain arrangement more preferable energetically than others.

Summing up, the energetically favored rotation for aligned pairs of identical heterochiral tubes is cog-wheel rotation or disrotation. For pairs of identical homochiral tubes, it is anti-cog-wheel rotation or conrotation that has the smallest barrier. There is a very low, 0.4-meV/Å, barrier to overcome if not conrotating the CNTs. For heterochiral pairs the barrier against disrotation is significantly larger, around 26.5 meV/Å. For the approximately 7-nm-long tubes considered presently even a few atoms excess or defect at the tube ending can destroy the energetic favor of conrotation of homochiral pairs. This effect of the tube ending certainly diminishes as the tube length increases. A similar phenomenon has been obtained by the calculations of Belikov *et al.*[29] on double wall CNTs, showing extremely small barriers to the relative rotation and sliding for certain tube pairs with commensurate walls.

The number of minima and maxima upon rotating one tube of an identical heterochiral (n,m) pair is $n+m$. Accordingly there are 20 minima and maxima along a horizontal or vertical line in Fig. 1. A homochiral pair of identical infinite (n,m) tubes shows $(n+m)/2$ minima upon rotating one of the tubes, as observable from Fig. 4(b). For achiral (n,n) and $(n,0)$ identical pairs the number of minima is $2n$ and n, respectively.

Figure 5 illustrates the $2n$ rule showing the potential curve of the $(10,10)||(10,10)$ pair, spanning two minima and two maxima. The two minima in Fig. 5 reminds to *AB* stacking observed in graphite. Of the two maxima the higher one is obtained at an *AA* like stacking. Apart from the minimum around 45°, *AB* like stacking is again apparent at minimal energy points on the rotational potential curve of the heterochiral $(12,8)||(12,8)$ pair shown in Fig. 6. A tendency to form *AB* like stacking has been used to interpret the stick-slip movement in experiments carried out with carbon nanotubes made to roll and slide on highly ordered pyrolytic graphite (HOPG) by AFM tips[30] and the preferential orien-

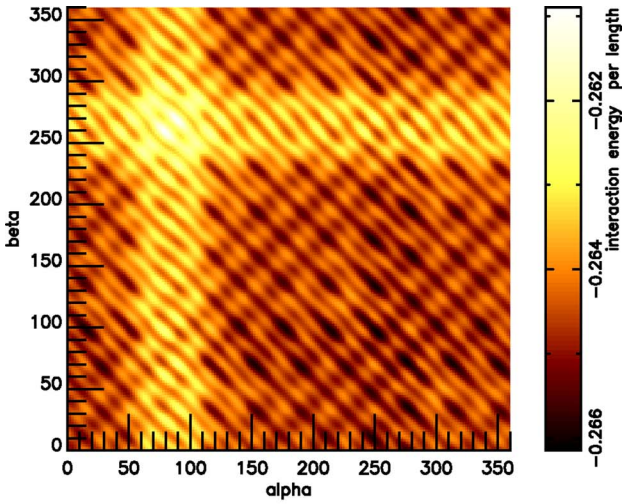

(a)

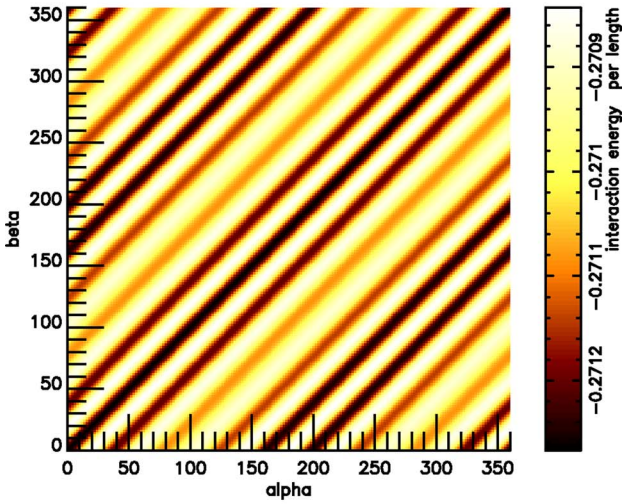

(b)

FIG. 4. (Color online) Rotational potential surface of two aligned (11,9) tubes, homochiral situation. Plot (a) shows a finite molecule treatment, plot (b) presents a calculation with periodic boundary conditions. There are 1202 (a) or 1204 (b) atoms per tube, wall to wall distance is 3.17 Å. Dimension of figures is eV/Å.

tation along three axes when depositing short carbon nanotubes onto HOPG from suspensions,[31] in accordance with the above calculations.

2. Pair interaction energies

In Table I interaction energies are collected for the pairs together with optimal wall to wall distances at the minimum and maximum energy orientation of the two tubes. Numbers in the table do not show a conspicuous preference for a certain CNT pair, minimal interaction energy of different pairs fall into the same range. However, small differences between minimal interaction energies of pairs can still be correlated with the experimental observation of homogeneous

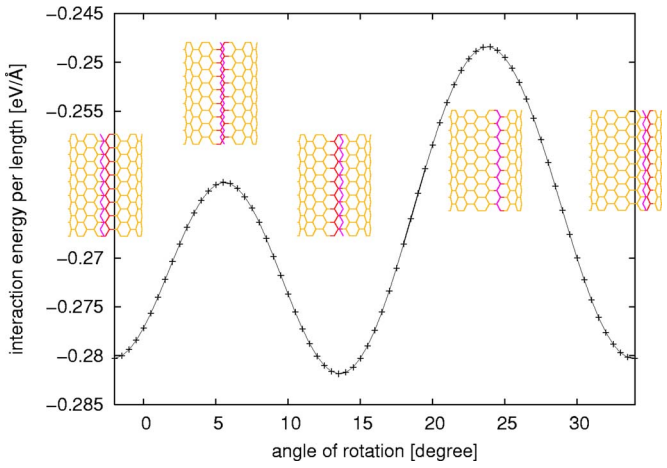

FIG. 5. (Color online) Interaction potential curve of two aligned (10,10) tubes with one tube fixed and the other rotating about its axis. Geometry at extremal points is shown in the inserted pictures. The fixed tube is halved in the inserts and only one zigzag line is shown of the other tube. The zigzag line of the moving tube and one zigzag line of the fixed tube is highlighted in the insets.

bundles.[11] Heterochiral identical pairs reported in Table I (indicated by superscript a) have the largest interaction energy. In addition, there are four nonidentical pairs (indicated by superscript b) which have the second largest interaction energies, in the range of −0.27 eV/Å. For two of these pairs [(11,9)||(15,4), *rl* and (15,4)||(12,8), *rl*] the difference of the chiral angles (15.2° and 12°) coincides with differences found experimentally in the case of SWCNT bundles grown by laser ablation.[11] The chirality difference of 21° for (12,8)||(17,1), *rl*, and 4° for (12,8)||(17,1), *rr*, does not show such a coincidence with experimental data, but one has to take into account that the number of studies in which the chirality distribution of SWCNT bundles has been analyzed in detail is extremely limited.

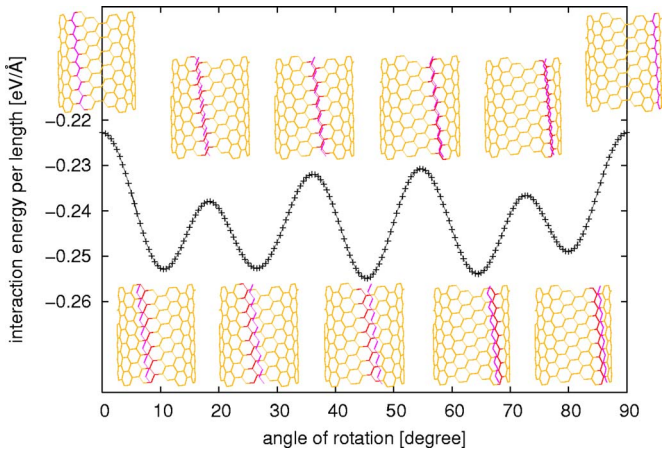

FIG. 6. (Color online) Interaction potential curve of two aligned (12,8) tubes with one tube fixed and the other rotating about its axis. Heterochiral situation. Geometry at extremal points is shown in the inserted pictures. The fixed tube is halved in the inserts and only one zigzag line is shown of the other tube. The zigzag line of the moving tube and one zigzag line of the fixed tube is highlighted in the insets.

TABLE I. Interaction energies per length and optimal wall to wall distances for aligned CNT pairs. Both quantities are tabulated at the minimum and maximum energy orientation (E_{min}, E_{max}, d_{min}, d_{max}). Corrugation of the surface is $E_{max}-E_{min}$. Tube lengths are 73.4 Å. Number of atoms per tube is 1220 for (10,10), 1202 for (11,9), 1196 for (15,4), 1208 for (12,8), 1204 for (17,1).

Tubes	E_{min} eV/Å	E_{max} eV/Å	$E_{max}-E_{min}$ meV/Å	d_{min} Å	d_{max} Å
(10,10)||(10,10)[a]	−0.2817	−0.2546	27.1	3.11	3.23
(10,10)||(11,9)	−0.2690	−0.2644	4.6	3.15	3.16
(10,10)||(15,4)	−0.2671	−0.2632	3.9	3.15	3.17
(10,10)||(12,8)	−0.2698	−0.2660	3.8	3.14	3.16
(10,10)||(17,1)	−0.2692	−0.2621	7.1	3.16	3.17
(11,9)||(11,9), *rl*[a]	−0.2770	−0.2501	26.9	3.11	3.22
(11,9)||(11,9), *rr*	−0.2669	−0.2615	5.4	3.15	3.16
(11,9)||(15,4), *rl*[b]	−0.2699	−0.2619	8.0	3.14	3.16
(11,9)||(15,4), *rr*	−0.2684	−0.2616	6.8	3.14	3.16
(11,9)||(12,8), *rl*	−0.2681	−0.2635	4.6	3.15	3.16
(11,9)||(12,8), *rr*	−0.2674	−0.2632	4.2	3.15	3.16
(11,9)||(17,1), *rl*	−0.2664	−0.2603	6.1	3.16	3.16
(11,9)||(17,1), *rr*	−0.2665	−0.2602	6.3	3.16	3.16
(15,4)||(15,4), *rl*[a]	−0.2767	−0.2490	27.7	3.11	3.22
(15,4)||(15,4), *rr*	−0.2642	−0.2597	4.5	3.15	3.17
(15,4)||(12,8), *rl*[b]	−0.2718	−0.2636	8.2	3.14	3.16
(15,4)||(12,8), *rr*	−0.2695	−0.2630	6.5	3.15	3.17
(15,4)||(17,1), *rl*	−0.2668	−0.2606	6.2	3.16	3.16
(15,4)||(17,1), *rr*	−0.2657	−0.2596	6.1	3.16	3.17
(12,8)||(12,8), *rl*[a]	−0.2791	−0.2531	26.0	3.11	3.22
(12,8)||(12,8), *rr*	−0.2682	−0.2642	4.0	3.15	3.16
(12,8)||(17,1), *rl*[b]	−0.2706	−0.2639	6.7	3.15	3.16
(12,8)||(17,1), *rr*[b]	−0.2703	−0.2641	6.2	3.15	3.16
(17,1)||(17,1), *rl*[a]	−0.2810	−0.2478	33.2	3.11	3.22
(17,1)||(17,1), *rr*	−0.2667	−0.2591	7.6	3.16	3.17

[a]Identical heterochiral (or achiral) CNT pairs.
[b]Nonidentical pairs with relatively large E_{min}.

Based on the largest corrugation of the rotational surface, heterochiral identical pairs are the most stable in the sense that they need the largest energy input to change the tube orientation (apart from disrotation). The largest corrugation of 27.2 meV/Å for the (10,10)||(10,10) pair is directly comparable with the 16.6-meV/Å maximum corrugation of the same surface computed by Kwon and Tománek.[14] Though there is a rough 2/3 factor between the two theoretical figures, it is confirming that the order of magnitude agrees. Better agreement is hard to expect regarding the differences in the models and their solution in the two studies.

Data computed for the experimentally observed tubes presented in Table II also reflect preference for heterochiral identical pairs. Interestingly the (12,6)||(12,6) pair has relatively small interaction energy. Of the three nonidentical complexes in Table II only the (10,10)||(13,7) pair shows interaction energy as large as obtained for heterochiral identical pairs.

TABLE II. Interaction energies per length and optimal wall to wall distances for aligned CNT pairs. See Table I for abbreviations. Tube lengths are 73.4 Å, number of atoms per tube is 1220 for (10,10), 1216 for (13,7), 1178 for (14,5), 1092 for (12,6), and 1142 for (10,9).

Tubes	E_{min} eV/Å	E_{max} eV/Å	$E_{max}-E_{min}$ meV/Å	d_{min} Å	d_{max} Å
(10,10)||(13,7)	−0.2701	−0.2644	5.7	3.15	3.17
(13,7)||(13,7), *rl*	−0.2792	−0.2499	29.3	3.11	3.23
(13,7)||(13,7), *rr*	−0.2677	−0.2621	5.6	3.15	3.17
(14,5)||(14,5), *rl*	−0.2752	−0.2464	28.8	3.11	3.23
(14,5)||(14,5), *rr*	−0.2630	−0.2570	6.0	3.15	3.17
(12,6)||(10,9), *rl*	−0.2569	−0.2535	3.4	3.15	3.16
(12,6)||(10,9), *rr*	−0.2568	−0.2535	3.3	3.15	3.16
(12,6)||(12,6), *rl*	−0.2681	−0.2426	25.5	3.10	3.22
(12,6)||(12,6), *rr*	−0.2569	−0.2536	3.3	3.15	3.16
(10,9)||(10,9), *rl*	−0.2710	−0.2452	25.7	3.11	3.22
(10,9)||(10,9), *rr*	−0.2612	−0.2570	4.2	3.15	3.16

Typical change in wall to wall distance when rotating a pair from an energetically preferred situation to a highly unpreferred one is around 0.01–0.02 Å. This falls into the same range as the calculated 0.03-Å radial deformation of tubes that arises due to tube-tube interaction.[32] The change in wall to wall distance for heterochiral identical pairs is an exception from the above rule, being an order of magnitude larger, around 0.1 Å.

B. Close-packed bundles of CNTs

As seen in Sec. III A, there is a small energetic favor in pairing identical achiral or identical heterochiral CNTs. Upon associating these tubes into bundles the energetic preference can get enlarged at an extent determined by the compatibility of the tube and the triangular lattice observed in bundles.[11]

1. Achiral tubes

Among all CNTs those that have a C_6 axis preserve symmetry elements of the triangular lattice. It is easy to point out that achiral tubes with a C_6 axis are not distinguished energetically, as they cannot fit in the lattice the best possible way. If one takes a seven-membered bundle of such tubes—accumulating 12 neighboring pair interactions—one may arrange at maximum nine pairs to reside at the most advantageous orientation, the remaining three necessarily occurring at the most disadvantageous facing in this case. This situation is illustrated in Fig. 7(a). On the other hand, achiral tubes with a C_3 axis may be arranged in the triangular lattice in such a way that all neighboring interactions are optimal, as shown in Fig. 7(b). The situation in Fig. 7(b) is achievable if minima on the pair rotational surface occur at $(\alpha_{min},\beta_{min})$ with β_{min} being halfway in between two α_{min}'s, i.e., $\beta_{min}=\alpha_{min}+60°$. In general achiral tubes possessing a C_{3n} axis with n even behave as illustrated in Fig. 7(a), while n being odd leads to an energetically optimal fitting into the lattice if

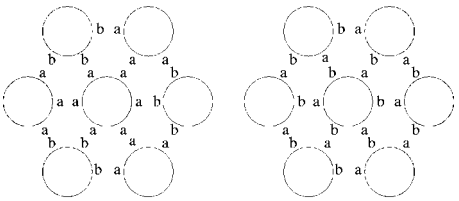

(a) (b)

FIG. 7. Facings at neighboring sites in seven-membered bundles of achiral CNTs possessing a C_{3n} axis. "a" labels the tube face found at α_{min}, "b" corresponds to the face at β_{min} with $(\alpha_{min}, \beta_{min})$ being the position of the minimum on the pair rotational potential surface. Situation (a) corresponds to n being even, (b) shows the case of n being odd.

$\beta_{min} = \alpha_{min} + 360° / (6n)$. This certainly holds not only for seven-membered bundles but for the entire triangular lattice.

Interaction energies and optimal wall to wall distances of seven-membered bundles of achiral tubes collected in Table III serve as an example of the above. The three columns of the table belong to three different categories: the C_9 axis of tube (9,9) is an odd multiple of 3, the C_{12} axis of tube (12,12) is an even multiple of 3 while the C_{10} axis of tube (10,10) is not divisible by 3. Optimal wall to wall distances in Table III show that (9,9) tubes may remain as close in bundle as they are in pairs. This is true neither for (12,12) nor for (10,10) tubes: they get away from each other by 0.01 or 0.02 Å, respectively, when a bundle is formed, indicating that the best facing cannot be formed for each neighbor.

The optimal 3.12-Å intertube separation for the (10,10) bundle is reasonably close to the theoretical value of 3.07 Å reported for the same system by Kwon *et al.*[32] Both numbers are somewhat smaller than 3.4 Å, observed by Thess *et al.*[33] and He *et al.*[34] The deviation is acceptable regarding that the experiment was performed at room temperature while calculations refer to zero K.

Interaction energies in Table III show an effect similar to intertube distance. For (9,9) tubes interaction energy of the seven-membered bundle is lower than the sum of 12 most favorable pair interactions by −0.008 eV/Å, due to the weak interaction of non-neighboring tubes. The deviation is opposite for (10,10) and (12,12) tubes, bundles having higher interaction energies than the sum of 12 pairs. The positive deviation is smaller for $n=12$ than for $n=10$ (0.013 eV/Å compared to 0.043 eV/Å) since most favorable neighboring interactions are more abundant in the (12,12) bundle. Interaction energy divided by the area of the interacting surface is −40.9 meV/Å^2 for $n=9$ while it is −37.8 meV/Å^2 for $n=10$ and −34.5 meV/Å^2 for $n=12$, again showing a small energetic favor of the (9,9) bundle. Interacting surface area is measured by the full area of the superficies of the middle tube plus six times one sixth of the superficies area of an outer tube, altogether two times the superficies area of a tube.

TABLE III. Optimal wall to wall distances in Å and interaction energies in eV/Å for pairs and bundles of (n,n) tubes, $n=9$, 10, 12. Rotation angles of the tubes are such that the interaction energy is at a local minimum on the hypersurface. Number of atoms constituting the tubes are 288 for $n=9$, 320 for $n=10$, and 384 for $n=12$. Tube lengths are 18.3 Å, corresponding to eight unit cells.

		(9,9)	(10,10)	(12,12)
Wall to wall distance	CNT pair	3.09	3.10	3.12
	7 membered bundle	3.09	3.12	3.13
Interaction energy	CNT pair	−0.259	−0.270	−0.293
	12 CNT pairs	−3.104	−3.244	−3.513
	7 membered bundle	−3.112	−3.201	−3.500

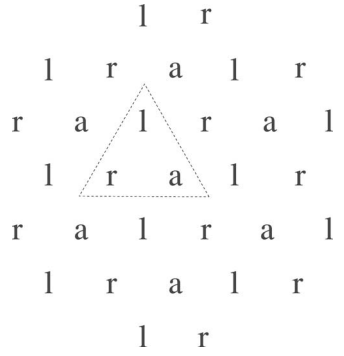

FIG. 8. Triangular lattice set with chiral tubes with a maximum possible opposite handedness facing. "l" indicates a left-handed tube, "r" stands for a right-handed tube, and "a" can be any of the two. A dashed triangle encloses the unit cell of the lattice.

The differences in interaction energies in Table III shows that certain bundles may be more stable than others. As this difference in stability increases with the length of the bundle, micron long bundles may have appreciable differences in their resistance to dispersion by ultrasonication or other procedures. This may have important implications in obtaining well dispersed SWCNT material which is a must for high quality composites based on carbon nanotubes.

2. Chiral tubes

Studying the bundle formation of chiral tubes one faces a situation complicated by the fact that opposite handedness pair interaction is favorable over same handedness. A honeycomb lattice of CNTs would be possible to fill exclusively with alternating heterochiral neighbors. This is, however, not possible for the triangular lattice. The maximum number of opposite handedness neighbors in the triangular lattice is obtained if setting a honeycomb lattice with alternating heterochiral neighbors, and putting additional CNTs in each middle of a hexagon. The handedness of these latter does not matter as they experience three *rl*-type and three *rr*-type pair interactions either way. A piece of such a lattice is shown in Fig. 8. It is interesting to note that in a lattice depicted in Fig. 8 it is possible to exercise such a rotation that every opposite handedness neighbors are disrotated and every same handedness neighbors are conrotated. As seen in Sec. III A these pair rotations have an extremely small barrier, such a rotation therefore is expected to require small energy input.

Due to the preference of opposite handedness neighbors, CNTs possessing a C_{3n} axis, with n being either even or odd, may fit into the lattice shown in Fig. 8 in an energetically

TABLE IV. Interaction energies per interacting surface area (E) in meV/Å^2 and optimal wall to wall distances of outer tubes (d) in Å of seven-membered close-packed bundles. Area of the interacting surface is measured by the averaged area of the superficies of the middle tube and an outer tube, to account for interactions of the middle tube. To this, interacting surface area of outer tubes among themselves is added, which is taken as six times one sixth of the superficies area of an outer tube, i.e., full superficies area of an outer tube. Right-handed middle CNT is denoted (n_1,m_1), alternating handedness outer CNTs are (n_2,m_2). Length of tubes is fixed at 69 Å, rotational angles correspond to a minimum on the rotational hypersurface.

(n_2,m_2)		(n_1,m_1)		
		(12,6)	(14,4)	(10,9)
(12,6)	E	−41.06	−39.28	−39.07
	d	3.11	3.26	3.28
(14,4)	E	−39.34	−39.63	−39.27
	d	3.05	3.12	3.15
(10,9)	E	−39.25	−39.48	−39.72
	d	3.04	3.11	3.13

optimal way. Among chiral (n,m) tubes that do not have a rotational axis one can distinguish those for which $n+m$ is divisible by 3. Supposing equidistant occurrence of minima on the rotational curve of the identical heterochiral pair, $n+m$ divisible by 3 generates better fitting into the lattice of Fig. 8 than $n+m$ not divisible by 3. (The divisibility requirement of $n+m$ by 3 is not related to the rule developed by Mintmire *et al.*[35] for metallic tubes.) Energetically worst fitting in the lattice would occur if there was a maximum on the pair rotational potential curve at some α_{min} (with β fixed at an arbitrary value), but a maximum at $\alpha_{min}+120°$. This, however, cannot happen, since there is either a minimum at $\alpha_{min}+120°$ (if $n+m$ is divisible by 3), or $\alpha_{min}+120°$ lies 1/3 way between two minima (if $n+m$ is not divisible by 3).

As an illustration, interaction energies normalized to unit interacting surface area are collected in Table IV for seven membered bundles. The outer six tubes are alternating heterochiral identical tubes, the type of CNT in the middle varies. Of the three tubes examined, (12,6) has a rotational axis of order divisible by 3 (C_6), for (14,4) $n+m=18$ is divisible by 3 and for (10,9) $n+m=19$ is not an integer multiple of 3. Interaction energies collected in the table are the largest in absolute value for the three homogeneous bundles. Bundles set with (14,4) or (10,9) CNTs have an interaction energy close to each other, while the (12,6) bundle has a definitely larger interaction energy, roughly −1 meV/Å^2 off from the other two. Interestingly, even (10,9) tubes, that provide example for the least well fitting tubes, form a six-membered bundle more stable than six best orientation tube pairs. This indicates that being 1/3 way off from the minimum on the pair rotational curve does not lead to a significant loss in interaction energy.

IV. CONCLUSION

It has been shown that there are rather small differences in interaction energies of aligned pairs of CNTs—suggesting a weak but significant energetic tube-tube preference in bundles. From pair rotational potential surfaces an energetically favorable rotation of identical tube pairs is apparent: conrotation for homochiral pairs and disrotation for achiral and heterochiral pairs. Intertube distance varies on the 10^{-2}-Å scale when changing tube orientation in aligned pairs. This variation gets enlarged to 10^{-1} Å in identical achiral or heterochiral pairs. Homogeneous bundles formed by achiral tubes have the largest interaction energy if the constituting tubes possess a C_{3n} axis with n an odd integer. A triangular lattice of chiral CNTs is suggested in which right- and left-handed tubes are distributed so that the maximum possible energetically preferred neigboring pair interactions can occur. In such a lattice (i) it is possible to change tube orientation so that each neighboring homochiral pairs conrotate and heterochiral pairs disrotate; (ii) those CNTs are preferred energetically, which possess a C_{3n} axis, n either even or odd, though this preference is again rather weak.

ACKNOWLEDGMENTS

This work has been partly supported by Grant No. OTKA D-45983-T-43685-T-49718-M-45294. The authors are indebted to the NIIF project for computational facilities.

*Email address: szabados@chem.elte.hu
†Email address: biro@mfa.kfki.hu
‡Email address: surjan@chem.elte.hu

[1] R. Saito, M. Fujita, G. Dresselhaus, and M. S. Dresselhaus, Appl. Phys. Lett. **60**, 2204 (1992).
[2] S. Ijima, Nature (London) **354**, 56 (1991).
[3] M-F. Yu, B. S. Files, S. Arepalli, and R. S. Ruoff, Phys. Rev. Lett. **84**, 5552 (2000).
[4] B. Vigolo, A. Pénicaud, C. Coulon, C. Sauder, R. Pailler, C. Journet, P. Bernier, and Ph. Poulin, Science **290**, 1331 (2000).
[5] L. M. Ericson, H. Fan, H. Peng, V. A. Davis, W. Zhou, J. Sulpizio, Y. Wang, R. Booker, J. Vavro, C. Guthy, A. N. G. Parra-Vasquez, M. J. Kim, S. Ramesh, R. K. Saini, C. Kittrell, G. Lavin, H. Schmidt, W. W. Adams, W. E. Billups, M. Pasquali, W-F. Hwang, R. H. Hauge, J. E. Fischer, and R. E. Smalley, Science **305**, 1447 (2004).
[6] M. Zhang, K. R. Atkinson, and R. H. Baughman, Science **306**, 1358 (2004).
[7] M. Zhang, S. Fang, A. A. Zakhidov, S. B. Lee, A. E. Aliev, Ch. D. Williams, K. R. Atkinson, and R. H. Baughman, Science **309**, 1215 (2005).
[8] K-T. Lau and D. Hui, Composites, Part B **33**, 2663 (2002).
[9] M. Radosavljevic, J. Lefebvre, and A. T. Johnson, Phys. Rev. B **64**, 241307(R) (2001).

[10] J.-F. Colomer, L. Henrard, Ph. Lambin, and G. Van Tendeloo, Phys. Rev. B **64**, 125425 (2001).
[11] J.-F. Colomer, L. Henrard, Ph. Lambin, and G. V. Tendeloo, Eur. Phys. J. B **27**, 111 (2002).
[12] L. P. Biró, J. Gyulai, Ph. Lambin, J. B. Nagy, S. Lazarescu, G. I. Márk, A. Fonseca, P. R. Surján, Zs. Szekeres, P. A. Thiry, and A. A. Lucas, Carbon **36**, 689 (1998).
[13] L. Henrard, E. Hernández, P. Bernier, and A. Rubio, Phys. Rev. B **60**, R8521 (1999).
[14] Y.-K. Kwon and D. Tománek, Phys. Rev. Lett. **84**, 1483 (2000).
[15] Y.-K. Kwon and D. Tománek, Phys. Rev. B **58**, R16001 (1998).
[16] A. H. R. Palser, Phys. Chem. Chem. Phys. **1**, 4459 (1999).
[17] A. Lázár, P. R. Surján, M. Paulsson, and S. Stafström, Int. J. Quantum Chem. **84**, 216 (2002).
[18] S. Tabor and S. Stafstrom, J. Magn. Magn. Mater. **104**, 2099 (1992).
[19] S. Stafstrom, Phys. Rev. B **47**, 12437 (1993).
[20] M. Paulsson and S. Stafstrom, Phys. Rev. B **60**, 7939 (1999).
[21] J. Kürti and P. R. Surján, Springer Ser. Solid-State Sci. **91**, 69 (1989).
[22] J. P. Doering, J. Chem. Phys. **51**, 2866 (1969).
[23] E. N. Lassettre, A. Skerbele, M. A. Dillon, and K. J. Ross, J. Chem. Phys. **48**, 5066 (1968).
[24] J. Kürti and P. R. Surján, J. Math. Chem. **10**, 313 (1992).
[25] P. R. Surján, A. Lázár, and M. Kállay, Phys. Rev. B **58**, 3490 (1998).
[26] P. R. Surján, A. Lázár, and Á. Szabados, Phys. Rev. A **68**, 062503 (2003).
[27] E. Bichoutskaia, A. M. Popov, A. El-Barbary, M. I. Heggie, and Y. E. Lozovik, Phys. Rev. B **71**, 113403 (2005).
[28] A. N. Kolmogorov and V. H. Crespi, Phys. Rev. Lett. **85**, 4727 (2000).
[29] A. V. Belikov, Yu. E. Lozovik, A. G. Nikolaev, and A. M. Popov, Chem. Phys. Lett. **385**, 72 (2004).
[30] M. R. Falvo, R. M. Taylor, A. Helser, V. Chi, F. P. Brooks, Jr., S. Washburn, and R. Superfine, Nature (London) **397**, 236 (1999).
[31] J. Liu, A. G. Rinzler, H. Dai, J. H. Hafner, R. K. Bradley, P. J. Boul, A. Lu, T. Iverson, K. Shelimov, C. B. Huffman, F. Rodriguez-Macias, Y-S. Shon, T. R. Lee, Daniel T. Colbert, and R. E. Smalley, Science **280**, 1253 (1998).
[32] Y-K. Kwon, D. Tománek, Y. H. Lee, K. H. Lee, and S. Saito, J. Mater. Res. **13**, 2363 (1998).
[33] A. Thess, R. Lee, P. Nikolaev, H. Dai, P. Petit, J. Robert, C. Xu, Y. H. Lee, S. G. Kim, D. T. Colbert, G. Scuseria, D. Tománek, J. E. Fischer, and R. E Smalley, Science **273**, 483 (1996).
[34] R. R. He, H. Z. Jin, J. Zhu, Y. J. Yan, and X. H. Chen, Chem. Phys. Lett. **298**, 170 (1998).
[35] J. W. Mintmire, B. I. Dunlap, and C. T. White, Phys. Rev. Lett. **68**, 631 (1992).
[36] M. Damnjanović, I. Milošević, T. Vuković, and R. Sredanović, Phys. Rev. B **60**, 2728 (1999).
[37] For curved surfaces such as tube walls, p_z orbitals are oriented towards the local normal direction of the surface.
[38] Damnjanović *et al.* (Ref. 36) use the notation (n_1,n_2) and (n_2,n_1) to specify optical isomers. In this study *r* and *l* is used for optical isomers (*P* or plus and *M* or minus according to the IUPAC nomenclature) to stress the role of handedness.